JACS
JOURNAL OF THE AMERICAN CHEMICAL SOCIETY
Article
pubs.acs.org/JACS

Catalytic CO_2 Activation Assisted by Rhenium Hydride/$B(C_6F_5)_3$ Frustrated Lewis Pairs—Metal Hydrides Functioning as FLP Bases

Yanfeng Jiang, Olivier Blacque, Thomas Fox, and Heinz Berke*

Anorganisch-chemisches Institut, Universität Zürich, Winterthurerstraß 190, CH-8037 Zürich, Switzerland.

Supporting Information

ABSTRACT: Reaction of **1** with $B(C_6F_5)_3$ under 1 bar of CO_2 led to the instantaneous formation of the frustrated Lewis pair (FLP)-type species $[ReHBr(NO)(PR_3)_2(\eta^2\text{-}O{=}C{=}O{-}B(C_6F_5)_3)]$ (**2**, R = *i*Pr **a**, Cy **b**) possessing two *cis*-phosphines and O_{CO_2}-coordinated $B(C_6F_5)_3$ groups as verified by NMR spectroscopy and supported by DFT calculations. The attachment of $B(C_6F_5)_3$ in **2a,b** establishes cooperative CO_2 activation via the Re−H/$B(C_6F_5)_3$ Lewis pair, with the Re−H bond playing the role of a Lewis base. The Re(I) η^1-formato dimer $[\{Re(\mu\text{-}Br)(NO)(\eta^1\text{-}OCH{=}O{-}B(C_6F_5)_3)(PiPr_3)_2\}_2]$ (**3a**) was generated from **2a** and represents the first example of a stable rhenium complex bearing two *cis*-aligned, sterically bulky $PiPr_3$ ligands. Reaction of **3a** with H_2 cleaved the μ-Br bridges, producing the stable and fully characterized formato dihydrogen complex $[ReBrH_2(NO)(\eta^1\text{-}OCH{=}O{-}B(C_6F_5)_3)(PiPr_3)_2]$ (**4a**) bearing *trans*-phosphines. Stoichiometric CO_2 reduction of **4a** with Et_3SiH led to heterolytic splitting of H_2 along with formation of bis(triethylsilyl)acetal ($(Et_3SiO)_2CH_2$, **7**). Catalytic reduction of CO_2 with Et_3SiH was also accomplished with the catalysts **1a,b**/$B(C_6F_5)_3$, **3a**, and **4a**, showing turnover frequencies (TOFs) between 4 and 9 h^{-1}. The stoichiometric reaction of **4a** with the sterically hindered base 2,2,6,6-tetramethylpiperidine (TMP) furnished H_2 ligand deprotonation. Hydrogenations of CO_2 using **1a,b**/$B(C_6F_5)_3$, **3a**, and **4a** as catalysts gave in the presence of TMP TOFs of up to 7.5 h^{-1}, producing [TMPH][formate] (**11**). The influence of various bases (R_2NH, R = *i*Pr, Cy, $SiMe_3$, 2,4,6-tri-*tert*-butylpyridine, NEt_3, $PtBu_3$) was studied in greater detail, pointing to two crucial factors of the CO_2 hydrogenations: the steric bulk and the basicity of the base.

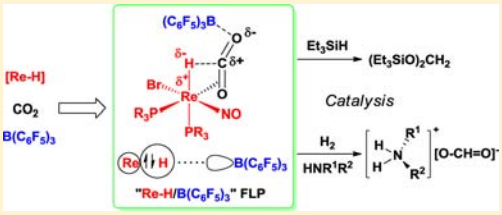

1. INTRODUCTION

CO_2 activation and reduction for alternative energy sources is a topic of current interest.[1] The major challenge originates from the high thermodynamic stability of CO_2, which calls for a remarkable driving force to ensure irreversible fixation. The currently developed chemical methods for CO_2 reduction could be classified into two categories based on either transition metals[2−4] or main-group elements[5−12] using dihydrogen,[2] hydrosilanes,[3] and boranes[4] as oxygen scavengers. One of the most prominent examples is the cooperative activation of CO_2 by frustrated Lewis pairs (FLPs), which consist of non-interacting or weakly interacting Lewis acid and base pairs of the B/P,[10] B/N,[11] or Al/P type.[12] FLPs are thus a milestone in the metal-free bifunctional activation of small molecules,[8,9] but in addition they provide a nonclassical way of activation using the polarizing power of electrostatic fields. In this context, the classical CO_2 insertion into a transition metal−hydride bond could be viewed as a bifunctional activation or a FLP-type activation process, showing for the former a vacant site at the metal center as the Lewis acid and for the latter the hydride as the Lewis base. The FLP arrangement actually emphasizes the crucial role of the hydride component, which must be hydridic and consequently nucleophilic in character to enable interaction with the electrophilic carbon atom of CO_2.[13]

In line with the FLP notion, we thus recognized that a transition metal−hydride bond can be taken as "isolobal" to the free electron pair of a Lewis base, as depicted schematically in Scheme 1. The shape of the σ orbital of a M−H bond with sufficiently hydridic character resembles that of the lone-pair electron of an organic Lewis base, which offers opportunity for activation by cooperation with an external Lewis acid to form a M−H/LA FLP. In addition, this structural arrangement would

Scheme 1. "Isolobal" Analogy between a Lewis Base and a Metal Hydride in the Bifunctional or FLP Activation Process of CO_2 (or Generally an XY Molecule): (Left) Classical CO_2 Bifunctional Activation by M−H and (Right) FLP-Type CO_2 Activation by a M−H/LA System with the M−H Unit as the Lewis Base Component

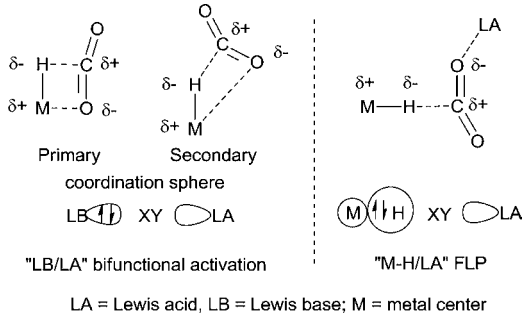

Received: March 7, 2013
Published: April 25, 2013

   dx.doi.org/10.1021/ja402381d | J. Am. Chem. Soc. 2013, 135, 7751−7760

allow subsequent reactivity with hydride transfer, as demonstrated by reports of Zr- and Ru-involved FLPs.[14] Based on this idea, this paper demonstrates that rhenium−hydride bonds can indeed act as a Lewis base in Re−H/B(C_6F_5)$_3$ FLPs to activate and reduce CO_2.

2. RESULTS AND DISCUSSION

2.1. Activation of CO_2 by the Re−H/B(C_6F_5)$_3$ Pair. The chemistry of the five-coordinate Re(I) hydride complexes [ReHBr(NO)(PR_3)$_2$] (**1**, R = *i*Pr **a**, Cy **b**) was developed particularly with respect to catalysis.[15] Due to its unsaturated 16e nature **1** shows strong affinities toward 2e donors, such as H_2, CO, O_2, ethylene, and carbenes.[15b] However, no reaction was observed when for instance the benzene-d_6 solution of **1a** or **1b** was exposed to 1 bar of CO_2 with spectroscopic monitoring. This reflected not only weak coordinating ability of CO_2, but maybe also insufficient hydridic and concomitant insufficient nucleophilic character of the Re−H bond for a secondary coordination sphere hydride transfer to CO_2. The position of the vacant site *trans* to the hydride also hampered the primary coordination sphere activation pathway. As verified additionally by ^{1}H, ^{31}P, and ^{19}F NMR spectroscopy, no reaction occurred between the pairs **1a**,**b** and B(C_6F_5)$_3$, or CO_2 and B(C_6F_5)$_3$.

In contrast, when the **1a**/B(C_6F_5)$_3$ or **1b**/B(C_6F_5)$_3$ mixtures (1:1) were exposed to 1 bar of CO_2 in benzene-d_6, the original purple solutions immediately turned light brown, affording within 20 min the six-coordinate 18e species **2** (R = *i*Pr **a**, Cy **b**) in 85% *in situ* yield, which were identified in solution as the Re(I) hydride structures of the type [ReHBr(NO)(PR_3)$_2$(η^2-O═C═O−B(C_6F_5)$_3$)] possessing two *cis*-phosphines and a B(C_6F_5)$_3$-attached η^2-CO_2 ligand (Scheme 2). The ^{1}H NMR spectrum revealed doublet of doublet resonances at 5.72 (**2a**) and 6.11 ppm (**2b**), which were assigned to the H_{Re} atoms. Surprisingly, two $^2J_{PH}$ coupling constants of 18 and 48 Hz were observed, which indicated the presence of phosphine ligands *cis* and *trans* to the hydride. In the ^{31}P NMR spectra, two doublets were observed at 39.6 and 33.0 ppm for **2a**, and at 30.0 and 22.1 ppm for **2b**. In comparison with the $^2J_{PP}$ values of ca. 120 Hz observable for *trans*-bisphosphine ligands, the relatively small coupling constants of ca. 80 Hz in **2** further supported *cis*-alignment of the two phosphine ligands.[15] The ^{1}H,^{31}P-correlation spectrum of **2a** recorded at −60 °C revealed only a correlation between the phosphorus signal at 39.6 ppm and that of the hydride, indicative of their *trans* positions. The other phosphorus signal at 33.0 ppm showed no correlation to the hydride, apparently suggesting their *cis* position. The ^{19}F NMR spectra exhibited a new set of resonances at −134.97 (*o*-F), −160.07 (*p*-F), −166.55 (*m*-F) ppm for **2a**, and at −134.16 (*o*-F), −159.99 (*p*-F), −166.47 (*m*-F) ppm for **2b**, providing evidence for the formation of the O−B(C_6F_5)$_3$ moiety.[16] In the long-range ^{13}C,^{1}H correlation spectrum of **2a** (HMBC), scalar couplings were observed between the hydride signal and the carbon resonances in the range from δ 150 to 135 ppm. This implied η^2 coordination of CO_2 *cis* to the Re−H bond, which enabled simultaneous interaction of the Re−H moiety with the C_{CO_2} atom and with the distantly coordinated B(C_6F_5)$_3$ moiety.

The CO_2 capture could be shown to be reversible, since exposure of the benzene solution of **2a**,**b** to N_2 or vacuum led to the quantitative regeneration of the free molecules **1a**,**b**, B(C_6F_5)$_3$, and CO_2, as evidenced for **1a**,**b** and B(C_6F_5)$_3$ by NMR spectroscopy. Addition of acetonitrile to the benzene solution of **2b** afforded instantaneously the CH_3CN·B(C_6F_5)$_3$ adduct, concomitant with the **1b**/CH_3CN adduct [ReHBr(NO)(PCy_3)$_2$(CH_3CN)],[15b] possessing two *trans*-phosphine ligands, further emphasizing the instability of **2a**,**b** envisaged to possess loosely bound CO_2.

The type **2** complexes appeared to be only intermittently stable even under 1 bar of CO_2 and gradually evolved into several new species within 4 h at 23 °C. The ^{1}H NMR spectrum then exhibited a new singlet at 9.61 ppm, which was correlated to a new singlet at 3.9 ppm in the ^{31}P NMR spectrum. The ^{19}F NMR spectrum revealed a new set of resonances at −133.62, −159.55, and −166.07 ppm. These were interpreted in terms of formation of a rhenium η^1-formato species with the terminal oxygen atom functionalized by B(C_6F_5)$_3$. This species was again seen to be transient and gradually transformed into two other species, revealing two singlets at 8.36 and 7.77 ppm in the ^{1}H NMR spectrum accompanied by two new singlets at 52.4 and 28.6 ppm in the ^{31}P NMR and two new sets of signals at −134.18, −159.32, −166.06 ppm and at −133.68, −158.82, −165.07 ppm in the ^{19}F NMR spectrum. Evidently, these data point to formation of two closely related rhenium formate isomers of as yet unknown detailed structures.

Interestingly, red-crystals gradually precipitated out from the benzene solution of **2a** along with the disappearance of **2a**. X-ray diffraction studies revealed a μ-Br-bridged Re(I) dimer η^1-formato structure [{Re(μ-Br)(NO)(η^1-OCH═O−B(C_6F_5)$_3$)($PiPr_3$)$_2$}$_2$] (**3a**) (Figure 1). Each center of the dimer adopts a pseudo-octahedral geometry. The B(C_6F_5)$_3$-coordinated formato moieties are located *trans* to the linear nitrosyl as a result of the strong π-donating/π-accepting push−pull effect. The most prominent structural feature is that the two phosphine ligands are *cis* showing a P−Re−P angle of 103.78(2)°. To the best of our knowledge, this is the first example of a *cis*-alignment of two sterically bulky $PiPr_3$ ligands within the realm of rhenium complexes. Rare cases of such pseudo-octahedral complexes with two *cis*-$PiPr_3$ ligands were observed previously in Os and Rh complexes.[17] Noteworthy is the fact that in the solid-state structure of **3a** the boron-attached C−O bond (1.268(3) Å) is longer than that bonded to the Re center

Scheme 2. CO_2 Insertion into the Re−H Bond of 1a,b with B(C_6F_5)$_3$[a]

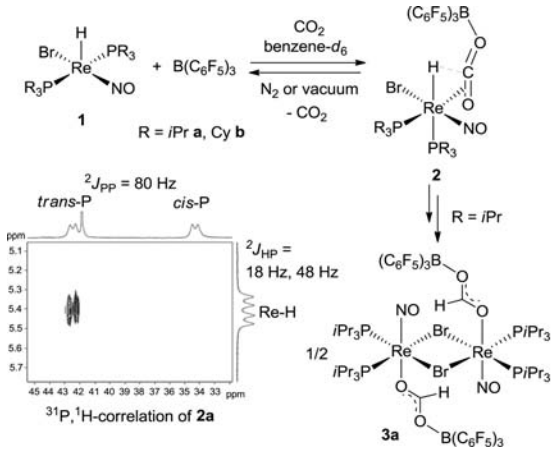

[a]The singlet observed in the ^{31}P NMR spectrum was assigned to unreacted **1a**.

dx.doi.org/10.1021/ja402381d | J. Am. Chem. Soc. 2013, 135, 7751−7760

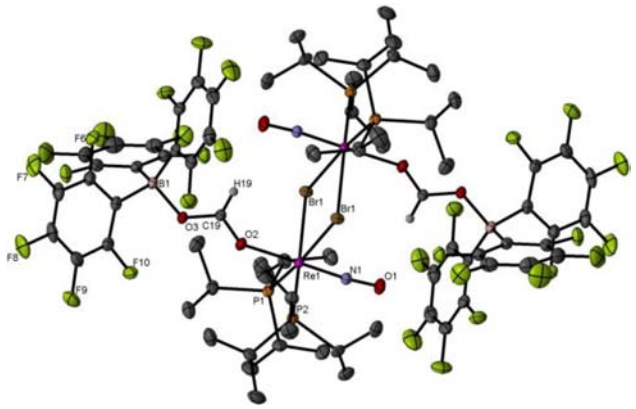

Figure 1. Molecular structure of **3a** with 30% probability displacement ellipsoids. All hydrogen atoms were omitted for clarity except for the formate moieties. Selected bond lengths (Å) and angles (deg): N(1)−O(1), 1.192(2); O(2)−Re(1), 2.1164(15); Re(1)−P(1), 2.4675(7); Re(1)−P(2), 2.4713(6); O(3)−B(1), 1.553(3); C(19)−O(2), 1.246(2); C(19)−O(3), 1.268(3); O(1)−N(1)−Re(1), 174.63(18); C(19)−O(2)−Re(1), 144.74(16); N(1)−Re(1)−O(2), 178.66(8); P(1)−Re(1)−P(2), 103.78(2); C(19)−O(3)−B(1), 126.52(18).

(1.246(2) Å), which is in accord with the conjugated character of the coordinated formato group characterized in solution.

Similarly, **2b** slowly evolved under CO_2 atmosphere at 23 °C into three new rhenium formate species showing singlets at 9.57, 8.36, and 8.14 ppm in the ^{1}H NMR spectrum, which are correlated to three singlets at 25.1, 20.2, and 7.0 ppm in the ^{31}P NMR spectrum. The species corresponding to the signal at 8.36 ppm remained as the major component after **2b** had completely disappeared within 15 h. In contrast to the case of **2a**, no precipitate was eventually formed. Particularly the ^{31}P NMR spectrum of the solution indicated a complex mixture, from which attempts to isolate stable products proved to be unsuccessful. We however assume that the reactions of **2b** proceeded along similar lines as that of **2a**.

Complex **3a** could be prepared in 72% isolated yield from the reaction of **1a**/$B(C_6F_5)_3$ (1:1.5) with 1 bar of CO_2 in benzene after stirring at 23 °C for 24 h. In the IR spectrum, the expected ν(NO) absorption is split, revealing bands at 1708 and 1695 cm^{-1}. The ν(OC═O) band was observed at 1592 cm^{-1}, which compared to Lewis acid-free [M−OCHO] species and is expected to have lowered ν(OC═O) wavenumbers due to π-electron withdrawal induced by the $B(C_6F_5)_3$ attachment.[18] For **3a** a satisfactory elemental analysis was obtained. NMR spectra of **3a** could not be recorded, due to insufficient solubility of this compound in non-coordinating solvents.

The structures of **2a**,**b** and related species along the CO_2 activation course were modeled by DFT calculations using PMe_3 model ligands. Based on the $[ReHBr(NO)(PMe_3)_2]$ system with *trans*- and *cis*-PMe_3 ligands (denoted as **transRe** or **cisRe**), the reactions with CO_2 and BF_3 were explored. All optimized structures were found to be local energy minima. The model of **2a**,**b** (**V**) shows a pseudo-pentagonal bipyramidal geometry with a Br−Re−NO axis (Figure 2). CO_2 is η^2-coordinated to the Re center, with BF_3 weakly attached to the O_{CO_2} atom showing a B−O distance of 1.633 Å. The relatively long Re−O distance of 2.243 Å speaks for a weakly bound CO_2 ligand, indeed consistent with the experimental observations for **2a**,**b**. The two PMe_3 ligands are disposed *cis* with a P−Re−P angle of 102.3°, which is quite comparable to that of the solid-state structure of **3a**.

The three free molecules of the **transRe**/CO_2/BF_3 arrangement **I** were taken as the energetic reference (0.0 kcal/mol). The energy of the mainly electrostatic binding of BF_3 to the Re−H bond in **II** was slightly endothermic (0.5 kcal/mol), showing a B−H bond distance of 2.341 Å. In the arrangement **II′** a B−O distance of 2.788 Å was observed, suggesting weak electrostatic interactions with −1.2 kcal/mol of released energy. The BF_3-functionalized CO_2 can weakly coordinate to **transRe**, showing in **V′** only −1.6 kcal/mol of stabilization energy. The two PMe_3 ligands are bent toward the hydride with a P−Re−P angle of 143.3°, which supposedly prevents the insertion of the

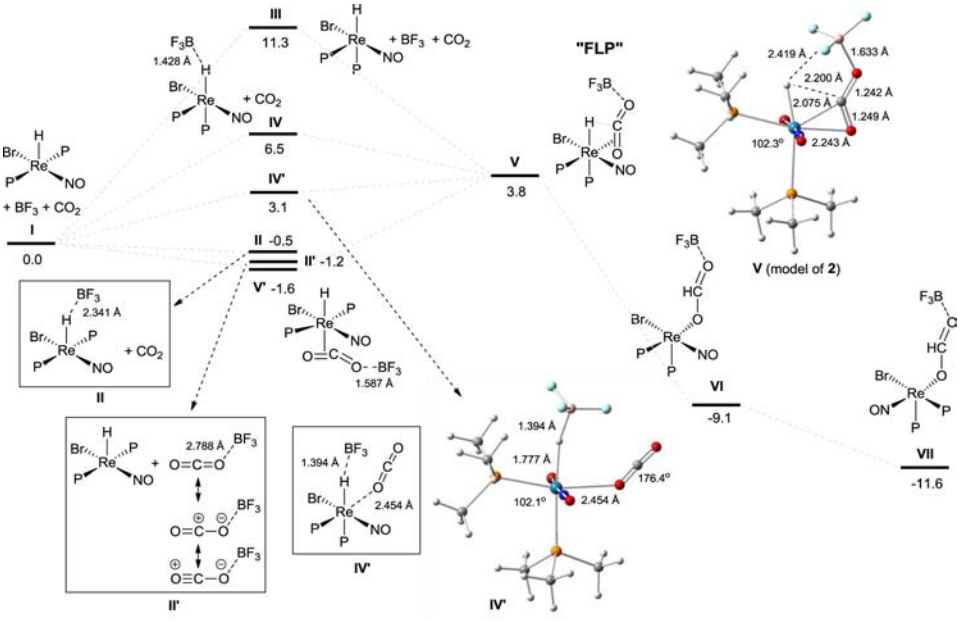

Figure 2. DFT-calculated intermediates possibly involved in the CO_2 activation course, with energies denoting local energy minima with respect to the reference (ΔE, kcal/mol).

dx.doi.org/10.1021/ja402381d | J. Am. Chem. Soc. 2013, 135, 7751−7760

C=O bond into the *trans* Re−H bond. On the other hand, the free **cisRe** molecule, CO_2, and BF_3 (**III**) are 11.3 kcal/mol higher in energy than the reference. The interaction between the BF_3 and the Re−H unit of **cisRe** is much stronger than that of **II** since a much shorter B−H distance of 1.428 Å was observed in **IV**, showing an energy decrease of 4.8 kcal/mol relative to **III**. Coordination of CO_2 to the Re center of **IV** resulted in **IV′**, which lies 3.4 kcal/mol lower in energy than **IV**. The interaction between BF_3 and the Re−H unit in **IV′** became further enhanced, showing a B−H distance of 1.394 Å. The CO_2 ligand remained linear and was weakly bound to the Re center, displaying a Re−O distance of 2.454 Å. Coordination of the BF_3-functionalized CO_2 to **cisRe** afforded **V**, which is 3.8 kcal/mol higher in energy than the reference and −7.5 kcal/mol below **III**. Following the activation course of CO_2 by Re−H and BF_3 further afforded the model formato species **VI**, releasing 12.9 kcal/mol in energy with respect to **V**. The isomerization of **VI** to **VII** bearing *trans*-aligned formato and nitrosyl ligands was found to be thermodynamically downhill by −2.5 kcal/mol. Furthermore, the dimerization via the bromo bridges led to a substantial thermodynamic stabilization of −15.5 kcal/mol.

On the basis of these calculational results, we are inclined to propose that substitution of BF_3 by $B(C_6F_5)_3$ would additionally support the geometry change from the *trans*-phosphine to the *cis*-phosphine arrangements. Subsequently cooperative activation of CO_2 by the Re−H···$B(C_6F_5)_3$ FLP occurs in a similar fashion as for the Stephan-type LB···$B(C_6F_5)_3$ FLPs by insertion of the substrate molecule between the Lewis pair encounter complex. Such an activation course could initially be assisted by an η^2-CO_2 π-type interaction with the rhenium center, which, similar to that in **V** or **V′**, helps to draw CO_2 closer to the Re−H and $B(C_6F_5)_3$ moieties.

2.2. Catalytic Reduction of CO_2 with Et_3SiH. The μ-Br bridges can be cleaved by 2e-donating molecules. For instance, under 1 bar of H_2 the suspension of **3a** in toluene afforded at 60 °C within 1 h the complex [$ReBrH_2(NO)(\eta^1$-OCH=OB$(C_6F_5)_3)(PiPr_3)_2$] (**4a**) in 99% isolated yield (Scheme 3). The

Scheme 3. Formation of the "Compressed Dihydride" Complex 4a and Its Subsequent Reaction with Et_3SiH

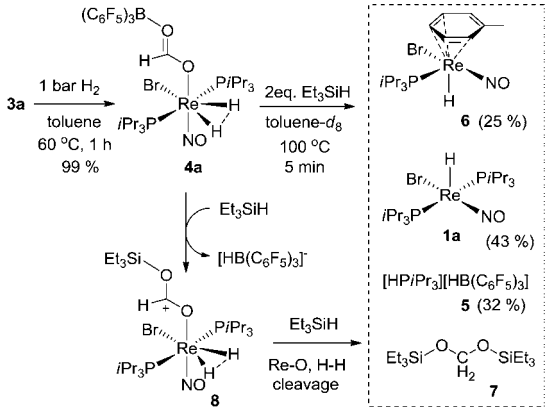

IR spectrum revealed two characteristic intense bands: a ν(NO) band at 1741 cm^{-1} and a ν(OC=O) band at 1595 cm^{-1}. The reaction with H_2 is assumed to lead to a "compressed dihydride" complex. The corresponding ^1H NMR resonance was observed as a relatively sharp triplet at 3.05 ppm, while the proton signal of the formato unit was found at 7.71 ppm in a typical region for $H_{formato}$ substituents. The ^{31}P NMR spectrum revealed a singlet resonance at 28.5 ppm, suggesting two chemically equivalent *trans*-phosphine ligands. The presence of a O−$B(C_6F_5)_3$ moiety was indicated by the set of signals at −134.81, −157.74, and −164.98 ppm in the ^{19}F NMR spectrum. As indicated by the ^1H NMR and by analogy to the reported dibromo dihydrogen Re(I) complexes,[19] the H_2 ligand in **4a** is anticipated to also belong to the class of "compressed dihydrides", with a considerably elongated, practically nonbonding H···H distance. This was supported further by DFT calculations on the model complex [$ReBrH_2(\eta^1$-OCH=O$BF_3)(NO)(PMe_3)_2$], where the H···H distance turned out to be nonbonding at 1.50 Å.

Addition of 2 equiv of Et_3SiH to the light yellow toluene solution of **4a** afforded at 100 °C after 5 min a purple mixture showing no trace of formato protons by ^1H NMR. Instead formation of the phosphonium borate [$HPiPr_3$][$HB(C_6F_5)_3$] (**5**)[20] was observed, exhibiting in the ^1H NMR spectrum a characteristic quartet of doublets signal at 4.40 ppm ($^1J_{HP}$ = 453 Hz), which correlated with a singlet at 42.6 ppm in the ^{31}P NMR spectrum, formed in 32% yield. The presence of the $[HB(C_6F_5)_3]^-$ anion of **5** was confirmed by both a doublet signal at −19.45 ppm in the ^{11}B NMR and the set of resonances at −134.19, −164.48, and −167.95 ppm in the ^{19}F NMR spectrum. Interestingly, a doublet signal at −7.61 ppm ($^2J_{HP}$ = 22 Hz) in the ^1H NMR spectrum could be spotted, which correlated with a phosphorus signal at 71.5 ppm in 25% yield. This signal was assigned to a monophosphine hydride moiety [$ReHBr(NO)(PiPr_3)$] presumably stabilized by an η^4-toluene ligand (**6**)[21] formed via heterolytic cleavage of the H−H bond in **4a** by dissociating a neighboring basic phosphine and deprotonating the H_2 ligand.[22] The ^{31}P NMR spectrum also revealed the formation of **1a** in 43% yield, which definitely indicated that cleavage of the Re−O bond in **4a** by Et_3SiH had occurred.

The ^{29}Si NMR spectrum revealed the presence of four silicon species showing singlets at 37.05, 30.01, 18.90, and 9.56 ppm. Among them the signal at 9.56 ppm was assigned to the [Et_3Si−H−$B(C_6F_5)_3$] adduct.[20] The resonance at 18.90 ppm represents the most prominent component, which corresponds to a singlet at 4.96 ppm in the ^1H NMR as revealed by the ^1H, ^{29}Si correlation spectrum. This evidently pointed to the formation of the bis(triethylsilyl)acetal $(Et_3SiO)_2CH_2$ (**7**), which was also observed by other CO_2 reduction systems using Et_3SiH as reducing agents, such as the Zr/$B(C_6F_5)_3$ system reported by Matsuo and Kawaguchi,[3b] the iridium pincer catalyst by Brookhart et al.,[3c] and the TMP/$B(C_6F_5)_3$ system by Piers et al.[11b] It is proposed that in a similar "tandem reaction" **4a** undergoes Et_3Si^+ replacement of $B(C_6F_5)_3$ to form the $[HB(C_6F_5)_3]^-$ and **8** (Scheme 3). The strong oxophilicity of the $[Et_3Si]^+$ cation attached to the O_{CO_2} atom weakens the Re−O bond in **8**, which then reacts further with Et_3SiH to afford **7**, accompanied by H−H heterolytic cleavage yielding **5** and **6**.

In an attempt to accomplish catalytic reduction of CO_2, we used the **1a**/$B(C_6F_5)_3$ system (1:1.5) and triethylsilane as a reductant under various conditions. In certain cases the silane functioned also as an oxygen scavenger (Table 1). Applying a catalyst loading of 1.0 mol% of **1a** and 1.5 mol% of $B(C_6F_5)_3$ in benzene-d_6 under 1 bar of CO_2 at 80 °C, 35% of the Et_3SiH was converted to $(Et_3SiO)_2CH_2$ (**7**) within 4 h, corresponding to a turnover number (TON) of 35 and a turnover frequency

dx.doi.org/10.1021/ja402381d | J. Am. Chem. Soc. 2013, 135, 7751−7760

Table 1. Catalytic Reduction of CO_2 by Et_3SiH

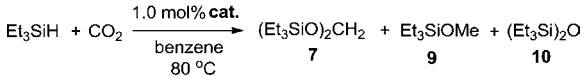

entry	catalyst	P_{CO_2} (bar)	t (h)	yield (%)[a] 7/9/10	TON	TOF (h^{-1})
1	**1a**/ $B(C_6F_5)_3$[b]	1	4	35/0/0	35	8.8
2	**1b**/ $B(C_6F_5)_3$[b]	1	4	18/0/0	18	4.5
3	**3a**	5	15	87/1/1	89	5.9
4	**4a**	5	13	89/3/3	95	7.3

[a]Determined by GC-MS. [b]In a ratio of 1:1.5.

(TOF) of 8.8 h^{-1}. In this experiment no other silyl-containing product could be observed by ^1H NMR spectroscopy.[3b,c,11b] GC-MS revealed the presence of small amounts of $(Et_3Si)_2O$, which however was anticipated to originate from the reaction of Et_3SiH with H_2O involved in the GC-MS manipulation. The **1b**/$B(C_6F_5)_3$ system proved to be less efficient, affording under the same conditions compound **7** with a TON of 18.

Significantly, the reaction catalyzed by 1 mol% of **4a** applying now 5 bar of CO_2 afforded at 80 °C within 13 h the silyl acetal **7** in 89% yield, which corresponds to a TON of 89 and a TOF of 6.8 h^{-1}. A very small amount (3%) of Et_3SiOCH_3 (**9**) was observed, which was recognized in the ^1H NMR spectrum as a singlet resonance at 3.32 ppm. We rationalized that **9** could be generated by the reaction of **7** with Et_3SiH. In addition the reaction produced $(Et_3Si)_2O$ (**10**) in amounts equivalent to **9**.[3b,c,11b] The catalytic reduction of CO_2 using 1 mol% of **3a** and Et_3SiH produced **7** within 15 h in 87% yield, corresponding to a TON of 87 and a TOF of 5.8 h^{-1}. Under the same conditions **3a** showed a slightly lower catalytic activity than **4a**, which was attributed to the lower solubility of **3a** in benzene. In the case of the catalysis with **3a**, product **9**, which requires an additional reduction step, was formed in only 1% yield together with an equivalent (1%) of **10**.

2.3. Catalytic CO_2 Hydrogenation in the Presence of Base. Catalytic hydrogenation of CO_2 was carried out with the **1**/$B(C_6F_5)_3$ system but additionally in the presence of the sterically hindered Lewis base 2,2,6,6-tetramethylpiperidine (TMP). Under 20 bar of CO_2 and 40 bar of H_2 in THF with 1 mmol of TMP, the **1a**/$B(C_6F_5)_3$ system (0.5 mol%, 1:2) afforded at 80 °C within 15 h the piperidinium formate salt [H-TMP]$^+$[O−CH═O]$^-$ (**11**) in 52% yield, corresponding to a TON of 104 (entry 2, Table 2). Formation of the related formamide could not be observed.[23] The same reaction afforded within 2 h a TON of 16, indicating a slow turnover rate (entry 3, Table 2). A blank reaction in the absence of **1**/$B(C_6F_5)_3$ did not afford hydrogenation at all (entry 4, Table 2). THF turns out to be an appropriate solvent for these catalyses, most probably due to its efficient solvation effect. The reaction in chlorobenzene or methanol showed under the same conditions lower activities (entries 1 and 12, Table 2). At 23 °C hydrogenation of CO_2 did not take place (entry 5, Table 2). Increasing the temperature to 120 °C resulted also in a poor TON (entry 6, Table 2), which was attributed to increased decomposition of the active species. Decreasing the H_2 and CO_2 pressures to 20 and 10 bar, respectively, resulted in a very small TOF (entry 7, Table 2), which was interpreted in terms of the inability to accumulate sufficient kinetically relevant concentrations of **4a**.

Table 2. Catalytic Hydrogenation of CO_2 in the Presence of TMP

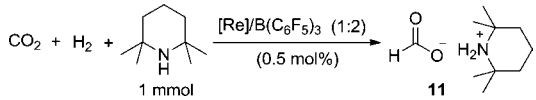

entry	[Re]	solvent	T (°C)	P_{H_2/CO_2} (bar)	t (h)	conv (%)[a]	TON	TOF (h^{-1})
1	**1a**	C_6H_5Cl	80	40/20	15	8	15	1.0
2	**1a**	THF	80	40/20	15	52[b]	104	6.9
3	**1a**	THF	80	40/20	2	8	16	7.5
4	–	THF	80	40/20	24	0	0	0
5	**1a**	THF	23	40/20	18	0	0	0
6	**1a**	THF	120	40/20	18	3	6	0.3
7	**1a**	THF	80	20/10	15	4	8	0.4
8	**1b**	THF	80	40/20	16	28	55	3.4
9[c]	**3a**	THF	80	40/20	15	36	72	4.8
10[c]	**4a**	THF	80	40/20	15	46	92	6.1
11[c]	**1a**	THF	80	40/20	15	39	78	5.2
12[c]	**1a**	MeOH	80	40/20	15	25	50	3.3

[a]Determined by referring to the internal standard DMF in ^1H NMR spectra. [b]In 20% isolated yield. [c]In the absence of $B(C_6F_5)_3$.

Remarkably, when **4a** was used as a catalyst in the absence of additional $B(C_6F_5)_3$, the hydrogenation of CO_2 in THF with 1 mmol of TMP at 80 °C afforded within 15 h a TON value of 92 (entry 10, Table 2), which is quite comparable to that of the **1a**/$B(C_6F_5)_3$ experiment. This indicated that complexes of type **4a** might be involved as intermediates in the various reaction courses. In comparison to **4a**, the activity of **3a** was found to be slightly lower, giving under the same conditions a TON of 72, presumably caused by the low solubility of **3a** in THF (entry 9, Table 2).

The molecular structure of **11** was established by both NMR spectroscopy and an X-ray diffraction study, as depicted in Figure 3. Moderately strong intermolecular hydrogen bonding was observed between the NH proton and the formate oxygen atom.[24]

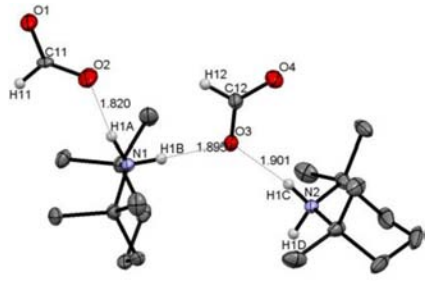

Figure 3. Molecular structure of **11** with 30% probability displacement ellipsoids. All hydrogen atoms are omitted for clarity except for the formate and NH_2 moieties.

To obtain further insight into the reaction mechanism, stoichiometric reactions of the catalyst were investigated. When **4a** was mixed with 2 equiv of TMP at 23 °C in THF-d_8, the solution instantaneously turned purple and a white precipitate formed. In the ^1H NMR spectrum a triplet resonance at −6.53 ppm (J_{HP} = 15 Hz) and a broad singlet at −15.22 ppm were observed, which correlated with two singlets at 41.8 and 40.8 ppm in the ^{31}P NMR spectrum. The triplet signal was assigned to a *trans*-diphosphine Re−H species generated via deproto-

dx.doi.org/10.1021/ja402381d | J. Am. Chem. Soc. 2013, 135, 7751−7760

nation of the H_2 moiety. The broad singlet at −15.22 ppm was characteristic for the hydride **1a**.[15a] Both observations implied TMP assisted H_2 heterolytic cleavage followed by dissociation of the formato ligand from the Re center of **4a**. The white precipitate could be ascertained to be the piperidinium formate **11**, which was partly still present in solution as confirmed by ^1H NMR spectroscopy. Products relating back to reactions with the TMP/$B(C_6F_5)_3$ FLP and CO_2 or H_2 could not be detected.[11,8]

The above results point to a CO_2 hydrogenation mechanism in the presence of $B(C_6F_5)_3$, as proposed in Scheme 4. Like in a FLP the activation pathway starts with the interaction of the hydride ligand of the **1**/$B(C_6F_5)_3$ pair with CO_2 to give **3**, which further reacts with H_2 to afford the formato dihydrogen complexes of type **4**. It should be noted at this point that the cycle is assumed to be driven by complexes with *trans*-phosphine arrangements. The *cis*-phosphine complexes of type **3** are assumed to function as resting states outside the catalytic cycle. In the presence of the sterically hindered Lewis base TMP, deprotonation of the H_2 ligand occurs, affording the [H-TMP]$^+$ cation and the anionic Re−H formato complex **12**, in full agreement with the observations of the described stoichiometric reaction.[22] **12** is prepared for formate elimination and exchange with H_2 via a 16e rhenium hydride species **13** to form **14**, since the π donor formate feels strong repulsion from the filled d orbitals of the rhenium center. The repulsion is even enhanced by the fact that the complex is anionic and loaded with charge. Subsequently the *trans*-dihydrogen hydride complex **14** is anticipated to rearrange to the isomeric "compressed dihydride" hydride **15** via a trihydride transition state.[25] Related rhenium complexes showed in H_2/D_2 scrambling experiments similar dihydrogen hydride exchange courses.[15e] DFT calculations using the [ReHBr(NO)$(PMe_3)_2$] model fragment suggest a practically thermoneutral process for the conversion of **13** to **14**, revealing the minute energy difference of −0.1 kcal/mol between the model complexes of **13**/H_2 and **14**. Similarly the isomerization step from **14** to **15** can be anticipated to be mildly "exothermic", since the calculations of the corresponding model complexes brought about a −6.0 kcal/mol energy difference.

Scheme 4. Sketch of a Catalytic Cycle for CO_2 Hydrogenation in the Presence of TMP, Displaying Compounds 1, 3, and 4 in the Presence and Absence of $B(C_6F_5)_3$[a]

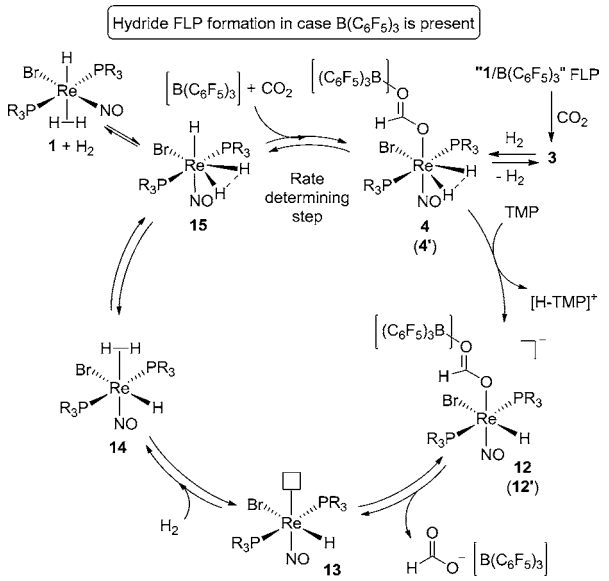

[a]Those species appearing in the absence of $B(C_6F_5)_3$ are denoted as **4′** and **12′**.

It should be noted at this point that H_2 ligands *trans* to a strong donor, like the hydride ligand, and *trans* to a strong π acceptor are expected to possess a H_2 ligand structure, while H_2 ligands *trans* to a π donor, like halogen ligands, should reveal an elongated dihydrogen or compressed dihydride structure.[26] In the catalytic reaction course **1** could possess higher concentrations similar to a resting state, since it precedes the rate-determining step.[15b] According to Scheme 4, **15** and $B(C_6F_5)_3$ constitute the catalytically crucial Re−H/$B(C_6F_5)_3$ FLP, which activates CO_2 and regenerates the type **4** complexes. The deprotonation step of **4** (**4′**) could principally be slow and rate determining, since the compressed dihydrides of type **4** are expected to be less acidic than dihydrogen complexes. Nevertheless, the stoichiometric deprotonation of **4a** proceeded instantaneously at ambient temperature, which indicates that the given compressed dihydrides are more acidic. Therefore, the regeneration step of **4** (**4′**) preceding the deprotonation is presumed to be rate determining. Earlier the stoichiometric reaction sequence of **1a**/$B(C_6F_5)_3$ with CO_2 and subsequently with H_2 was shown to be overall very slow at room temperature. The related transformation, which constitutes insertion of CO_2 into the Re−H bond, is expected to be slow even at the higher temperature of 80 °C of the catalyses. Therefore, we rationalized that this step would be the slowest of all steps of the catalytic cycle and rate determining.

It should also be noted that the **1**/$B(C_6F_5)_3$/CO_2/H_2 reaction mixture contains not only the **1**/$B(C_6F_5)_3$ FLP but also the "classical" metal-free TMP/$B(C_6F_5)_3$ FLP. Competitive FLP reactivity can be envisaged to occur with simultaneous capture of CO_2 and H_2 by this FLP, leading to the formation of a [H-TMP][O═CH−O$B(C_6F_5)_3$] product, or by H_2 embracement to the [H-TMP][H$B(C_6F_5)_3$] salt.[11,8] In the presence of **1a**, however, these FLP reaction channels seemed not to be competitive with the reactions of the **1**/$B(C_6F_5)_3$ FLP, as implied by entry 4 in Table 2.

The potential of the catalytic CO_2 hydrogenation applying **1a** was additionally explored in the absence of $B(C_6F_5)_3$, which surprisingly afforded under the same conditions as in the presence of $B(C_6F_5)_3$ a TON of 78 (entry 11, Table 2). Thus, **1a** alone appeared to be a good but somewhat less active catalyst than the co-catalytic system **1a**/$B(C_6F_5)_3$. We assume that this catalysis follows a similar reaction course with formation of the $B(C_6F_5)_3$ free formato rhenium species **4′**. The secondary coordination sphere hydride transfer from **15** onto CO_2 does not contrast the observation that **1** does not react with CO_2, since the reactive species **14** are isomeric to **1**. Structures of type **14** are expected to possess a more hydridic character in the Re−H bonds than **1**, which originates from the *trans* influence of the *trans*-positioned NO ligand. The H_2 ligand of **4′** is however expected to be less acidic than that of **4**, since the $B(C_6F_5)_3$ substituent of **4** leads to additional electron withdrawal, affecting also the H_2 ligand.

In a tuning effort different bases of various base strengths were then tested for their performance in the hydrogenation of CO_2. Exclusive formation of the corresponding formate salts was invariably observed instead of the alternative formation of formamide compounds (Table 3). In the case of the sterically

dx.doi.org/10.1021/ja402381d | J. Am. Chem. Soc. 2013, 135, 7751−7760

Table 3. Comparison of the Performance of Different Bases in Catalytic Hydrogenation of CO_2

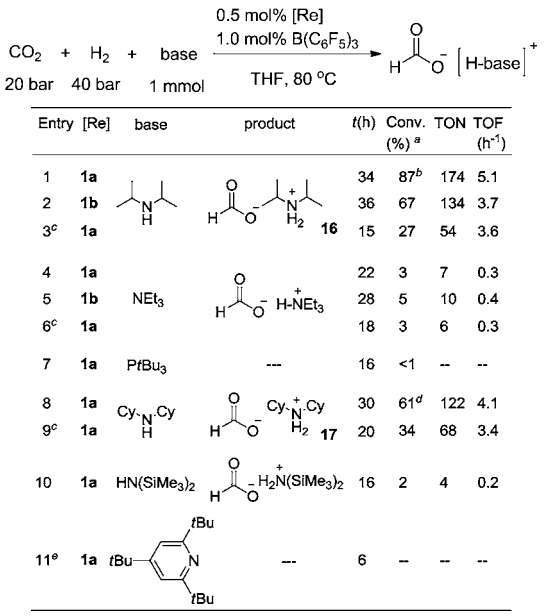

Entry	[Re]	base	product	t(h)	Conv. (%) [a]	TON	TOF (h^{-1})
1	**1a**			34	87[b]	174	5.1
2	**1b**		**16**	36	67	134	3.7
3[c]	**1a**			15	27	54	3.6
4	**1a**			22	3	7	0.3
5	**1b**	NEt_3	$H\text{-}NEt_3^+$	28	5	10	0.4
6[c]	**1a**			18	3	6	0.3
7	**1a**	$PtBu_3$	---	16	<1	--	--
8	**1a**	Cy_2NH	**17**	30	61[d]	122	4.1
9[c]	**1a**			20	34	68	3.4
10	**1a**	$HN(SiMe_3)_2$	$H_2N^+(SiMe_3)_2$	16	2	4	0.2
11[e]	**1a**	2,4,6-tri-*tert*-butylpyridine	---	6	--	--	--

[a]Determined by referring to the internal standard DMF in ^1H NMR spectra. [b]In 12% isolated yield. [c]In the absence of $B(C_6F_5)_3$. [d]In 13% isolated yield. [e]With 10 mol% of **1a**/$B(C_6F_5)_3$ (1:2).

less demanding base $HNiPr_2$, the catalytic system of **1a**/$B(C_6F_5)_3$ afforded the formate salt $[HNiPr_2]^+[O{-}CH{=}O]^-$ (**16**) within 34 h in 87% yield, corresponding to a TON of 174 and a TOF of 5.1 h^{-1} (entry 1, Table 3). The **1b**/$B(C_6F_5)_3$ system was found here to be slightly less active. Within 36 h a TON of 134 was accomplished (entry 2, Table 3). The reaction with the least bulky amine NEt_3 afforded under the same conditions poorer TONs of up to 10 within 28 h (entries 4 and 5, Table 3). By comparison, $HNCy_2$ as a base furnished a conversion of 61% and a TON of 122 using the **1a**/$B(C_6F_5)_3$ co-catalytic system with formation of the $[HNCy_2]^+[O{-}CH{=}O]^-$ (**17**) salt (entry 8, Table 3). These results evidently pointed out that steric hindrance of the employed base is key to the efficiency of the CO_2 hydrogenation. Another crucial factor is apparently the basicity of the base. In the case of $PtBu_3$, which is sterically bulky, but much less basic than the secondary amines, nearly no catalytic activity was observed (entry 7, Table 3). The NMR spectrum revealed a complex mixture possibly containing the CO_2-captured product $[tBu_3P{-}C(=O){-}O{-}B(C_6F_5)_3]$ originating from the reaction of CO_2 with the $PtBu_3/B(C_6F_5)_3$ FLP.[10a] However, the H_2-activated product $[HPtBu_3][HB(C_6F_5)_3]$ was not observed. The crucial role of the basicity of the base was further supported by the reaction using $HN(SiMe_3)_2$, which is bulkier but less basic than $HNiPr_2$. Indeed, a very poor TON of 4 was obtained within 16 h under the same catalytic conditions as for the other base reactions (entry 10, Table 3). 2,4,6-Tri-*tert*-butylpyridine also showed no conversion in the CO_2 hydrogenation, attributed to its too low basicity (entry 11, Table 3). Finally, it should be mentioned that in all cases of secondary amines the CO_2 hydrogenations catalyzed by **1a** were also examined in the absence of $B(C_6F_5)_3$. Invariably inferior catalytic performances compared to those in the presence of $B(C_6F_5)_3$ were observed.

3. CONCLUSIONS

In conclusion, we demonstrated that cooperative FLP-type activation of CO_2 can be accomplished by Re−H/$B(C_6F_5)_3$ systems with the Re−H bond operating as the Lewis base component. These FLPs rendered subsequent catalytic reduction of CO_2 by a hydrosilane and catalytic hydrogenation of CO_2 in the presence of sterically hindered strong bases. This work therefore not only emphasized the possibility for extending the scope of the FLP concept to transition metal hydrides as base components to get involved in small-molecule activations, but also demonstrated that FLP tuning of non-platinum-group transition metals may provide ample opportunity for catalytic CO_2 reduction. Explorations of related but more efficient catalytic CO_2 hydrogenation processes are currently underway in our group.

4. EXPERIMENTAL SECTION

General Experimental. All manipulations were carried out under an atmosphere of dry nitrogen using standard Schlenk techniques or in a glovebox (M. Braun 150B-G-II) filled with dry nitrogen. Solvents were freshly distilled under N_2 by employing standard procedures and were degassed by freeze−thaw cycles prior to use. The deuterated solvent CD_2Cl_2 was dried over molecular sieves, whereas benzene-d_6 and toluene-d_8 were dried with sodium/benzophenone and vacuum-transferred for storage in a Schlenk flask fitted with Teflon valves. ^1H NMR, $^{13}C\{^1H\}$ NMR, $^{31}P\{^1H\}$ NMR, ^{19}F NMR, and ^{11}B NMR data were recorded on a Varian Mercury 300 spectrometer using 5 mm diameter NMR tubes equipped with Teflon valves, which allow degassing and further introduction of gases into the probe. Chemical shifts are expressed in parts per million (ppm). ^1H and $^{13}C\{^1H\}$ NMR spectra were referenced to the residual proton or ^{13}C resonances of the deuterated solvent. All chemical shifts for the $^{31}P\{^1H\}$ NMR data are reported downfield in ppm relative to external 85% H_3PO_4 at 0.0 ppm. Signal patterns are reported as follows: s, singlet; d, doublet; t, triplet; m, multiplet. IR spectra were obtained by using ATR methods with a Bio-Rad FTS-45 FTIR spectrometer. Complexes **1** were prepared according to reported procedures.[15a]

[{Re(μ-Br)(NO)(η^1-OCH=OB(C_6F_5)$_3$)($PiPr_3$)$_2$}$_2$] (3a). In a 30 mL Young-tap Schlenk vessel, 62.0 mg of $[ReHBr(NO)(PiPr_3)_2]$ (**1a**, 0.10 mmol) was mixed in a glovebox with 71.5 mg of $B(C_6F_5)_3$ (0.14 mmol) in 5 mL of benzene. The N_2 atmosphere was replaced with 1.0 bar of CO_2 using a freeze−pump−thaw cycle. After warming to room temperature, the originally violet solution instantaneously turned brown. The mixture was kept stirring at room temperature overnight, leading to the formation of a large amount of a pale-red precipitate, which was isolated, further washed with benzene (1 × 1 mL) and pentane (3 × 3 mL), and dried *in vacuo* to afford a pale-red solid: 84.0 mg, 72% yield. IR (cm^{-1}, ATR): ν (NO) 1708, 1695; ν (OC=O) 1592. Anal. Calcd for $C_{74}H_{86}B_2Br_2F_{30}N_2O_6P_4Re_2$ (2347.18): C, 37.87; H, 3.69; N, 1.19. Found: C, 37.48; H, 3.85; N, 1.09.

Reaction of 1a with $B(C_6F_5)_3$ and CO_2 in the NMR Tube. In a 3 mL Young-tap NMR-tube, 12.4 mg of **1a** (0.02 mmol) was mixed with 30.2 mg of $B(C_6F_5)_3$ (0.06 mmol, 3 equiv) in 0.6 mL of benzene-d_6 to give a deep-purple solution. Although the ^{19}F NMR spectrum implied the presence of free $B(C_6F_5)_3$, the ^{31}P NMR resonance at 43.4 ppm became broadened, and the Re−H resonance in the ^1H NMR spectrum disappeared. This all indicated a weak interaction between the Re−H and the boron atom of $B(C_6F_5)_3$ in solution. Formate formation was not observed. The N_2 atmosphere was then replaced with 1.0 bar of CO_2 using a freeze−pump−thaw cycle. The purple solution turned immediately brown. After 20 min, ^{31}P NMR spectroscopy confirmed formation of the intermediate species **2a** in 85% yield as the only new species. ^1H NMR (300.08 MHz, benzene-d_6, ppm): δ 5.72 (dd, $^2J_{(HP)}$ = 48 Hz, $^2J_{(HP)}$ = 18 Hz, 1H, ReH), 2.75 (m, 3H, PCH(CH$_3$)$_2$), 2.50 (m, 3H, PCH(CH$_3$)$_2$), 1.31 (m, 9H, PCH(CH_3)$_2$), 1.12 (m, 9H, PCH(CH_3)$_2$), 0.93 (m, 18H, PCH-(CH_3)$_2$). $^{13}C\{^1H\}$ NMR (75.47 MHz, benzene-d_6, ppm): δ 27.1 (d,

dx.doi.org/10.1021/ja402381d | J. Am. Chem. Soc. 2013, 135, 7751−7760

$J_{(PC)}$ = 28 Hz, P-CH), 24.6 (d, $J_{(PC)}$ = 24 Hz, P-CH), 19.2 (s), 19.1 (s), 18.3 (m), 18.0 (s). $^{31}P\{^1H\}$ NMR (121.47 MHz, benzene-d_6, ppm): δ 39.62 (d, $^2J_{(PP)}$ = 84 Hz, 1P), 33.05 (d, $^2J_{(PP)}$ = 82 Hz, 1P). ^{19}F NMR (282.33 MHz, benzene-d_6, ppm): δ −134.97 (m, 6F, *ortho*-C_6F_5), −160.07 (t, $^1J_{CF}$ = 20 Hz, 3F, *para*-C_6F_5), −166.55 (m, 6F, *meta*-C_6F_5). No signals were observed in ^{11}B NMR spectroscopy.

Reaction of 1b with $B(C_6F_5)_3$ and CO_2 in the NMR Tube. In a 3 mL Young-tap NMR tube, 17.2 mg of **1b** (0.02 mmol) was mixed with 30.1 mg of $B(C_6F_5)_3$ (0.06 mmol, 3 equiv) in 0.6 mL of benzene-d_6 to give a deep-purple solution. ^1H, ^{31}P, and ^{19}F NMR spectroscopy indicated that reaction had not occurred between **1b** and $B(C_6F_5)_3$, as the original resonances (for instance Re−H signal at −17.0 ppm in the ^1H NMR) still remained, and no new species formed. The N_2 atmosphere was then replaced with 1.0 bar of CO_2 using a freeze−pump−thaw cycle. Immediately the purple solution turned light brown, indicative of formation of the 18e rhenium species **2b**. After 30 min, ^{31}P NMR spectroscopy confirmed the quantitative formation of **2b**. Formate was not generated at this stage. ^1H NMR (300.08 MHz, benzene-d_6, ppm): δ 6.11 (dd, $^2J_{(HP)}$ = 48 Hz, $^2J_{(HP)}$ = 18 Hz, 1H, ReH), 1.03−2.70 (m, 66H, $P(C_6H_{11})_3$). $^{13}C\{^1H\}$ NMR (75.47 MHz, benzene-d_6, ppm): δ 37.2 (d, $J_{(PC)}$ = 26 Hz, P-CH), 33.9 (d, $J_{(PC)}$ = 23 Hz, P-CH), 29.6 (s), 29.0 (s), 27.5 (m), 27.0 (s), 26.2 (s). $^{31}P\{^1H\}$ NMR (121.47 MHz, benzene-d_6, ppm): δ 30.00 (d, $^2J_{(PP)}$ = 79 Hz, 1P), 22.13 (d, $^2J_{(PP)}$ = 79 Hz, 1P). ^{19}F NMR (282.33 MHz, benzene-d_6, ppm): δ −134.16 (m, 6F, *ortho*-C_6F_5), −159.99 (t, $^1J_{CF}$ = 22 Hz, 3F, *para*-C_6F_5), −166.47 (m, 6F, *meta*-C_6F_5). ^{11}B NMR signals could not be observed. The transient species is only temporarily stable under CO_2 atmosphere. Exposure of the solution to vacuum leads to back-reaction affording the starting materials **1b**/$B(C_6F_5)_3$ in over 90% yield.

Addition of 5 drops of acetonitrile to the benzene solution of the intermediate led to the quantitative formation of the *trans*-phosphine Re(I) hydride species $[ReHBr(NO)(PCy_3)_2(CH_3CN)]$[15b] ($^{31}P$ NMR: δ 16.6 ppm) and $CH_3CN{\cdot}B(C_6F_5)_3$ (^{19}F NMR in benzene-d_6: δ −130.84 (m, 6F, *ortho*-C_6F_5), −151.68 (t, $^1J_{CF}$ = 20 Hz, 3F, *para*-C_6F_5), −159.48 (m, 6F, *meta*-C_6F_5); ^{19}F NMR in CD_2Cl_2: δ −136.22 (m, 6F, *ortho*-C_6F_5), −158.74 (t, $^1J_{CF}$ = 20 Hz, 3F, *para*-C_6F_5), −165.92 (m, 6F, *meta*-C_6F_5)).

$[ReBrH_2(NO)(\eta^1\text{-}OCH{=}OB(C_6F_5)_3)(PiPr_3)_2]$ (4a). In a 30 mL Young-tap Schlenk vessel placed in a glovebox, 60 mg of **3a** (0.025 mmol) was mixed in 2 mL of toluene. The N_2 atmosphere was replaced with 1.0 bar of H_2 using a freeze−pump−thaw cycle. The mixture was kept at 60 °C for 1 h, affording a clear, light brown solution. After filtration through Celite, the solvent was evaporated *in vacuo*, and the residue was washed with pentane (3 × 2 mL) and dried, giving a light brown solid: 61 mg, 99%. IR (cm^{-1}, ATR): ν (NO) 1741, ν (OC=O) 1595. ^1H NMR (300.08 MHz, toluene-d_8, ppm): δ 7.71 (s, 1H, OCHO), 3.05 (t, $^2J_{(HP)}$ = 18 Hz, 2H, η^2-H_2), 2.20 (m, 6H, $PCH(CH_3)_2$), 1.15 (m, 18H, $PCH(CH_3)_2$), 0.82 (m, 18H, $PCH(CH_3)_2$)). $^{13}C\{^1H\}$ NMR (75.47 MHz, toluene-d_8, ppm): δ 173.0 (s, OCHO), 150.3 (s), 147.1 (s), 139.0 (s), 136.2 (s), 23.6 (t, $J_{(PC)}$ = 12 Hz, P-CH), 18.6 (s, $PCH(CH_3)_2$). $^{31}P\{^1H\}$ NMR (121.47 MHz, toluene-d_8, ppm): δ 28.5 (s). ^{19}F NMR (282.33 MHz, toluene-d_8, ppm): δ −134.81 (m, 6F, *ortho*-C_6F_5), −157.74 (t, $^1J_{CF}$ = 20 Hz, 3F, *para*-C_6F_5), −164.98 (m, 6F, *meta*-C_6F_5). Anal. Calcd for $C_{37}H_{45}BBrF_{15}NO_3P_2Re$ (1175.60): C, 37.80; H, 3.86; N, 1.19. Found: C, 38.01; H, 3.74; N, 1.11.

Reaction of 4a with Et_3SiH. In a 3 mL Young-tap NMR-tube, 12 mg of **4a** (0.01 mmol) was mixed with 3.2 μL of Et_3SiH (0.02 mmol) in 0.6 mL of toluene-d_8. After being kept at 100 °C for 5 min, the solution turned from light brown to bright pink. NMR spectroscopy indicated the disappearance of the starting materials (absence of a formate OCHO signal at 7.7 ppm) and the formation of several species:

$[HPiPr_3][HB(C_6F_5)_3]$ ***(5, 32%).*** ^1H NMR (300.08 MHz, toluene-d_8, ppm): δ 4.40 (dxq, 1H, $^3J_{HH}$ = 6 Hz, $^1J_{HP}$ = 453 Hz, PH). $^{31}P\{^1H\}$ NMR (121.47 MHz, toluene-d_8, ppm): δ 42.6 (s). ^{11}B NMR (96.28 MHz, toluene-d_8, ppm): δ −19.45 (d, $^1J_{HB}$ = 96 Hz). ^{19}F NMR (282.33 MHz, toluene-d_8, ppm): δ −134.19 (m, 6F, *ortho*-C_6F_5), −164.48 (m, 3F, *para*-C_6F_5), −167.95 (m, 6F, *meta*-C_6F_5).

1a* *(43%). Characterized by its purple color in solution. $^{31}P\{^1H\}$ NMR (121.47 MHz, toluene-d_8, ppm): δ 41.1 (s).

$[ReHBr(NO)(PiPr_3)(\eta^4\text{-toluene})]$ ***(6, 25%).*** ^1H NMR (300.08 MHz, toluene-d_8, ppm): δ −7.61 (d, 1H, $^2J_{HP}$ =22 Hz, ReH). $^{31}P\{^1H\}$ NMR (121.47 MHz, toluene-d_8, ppm): δ 71.5 (s).

$(Et_3SiO)_2CH_2$ ***(7).*** ^1H NMR (300.08 MHz, toluene-d_8, ppm): δ 4.96 (s). ^{19}F NMR (282.33 MHz, toluene-d_8, ppm): δ −134.19 (m, 6F, *ortho*-C_6F_5), −159.81 (m, 3F, *para*-C_6F_5), −164.76 (m, 6F, *meta*-C_6F_5).

Reduction of CO_2 with Et_3SiH Catalyzed by 1a/$B(C_6F_5)_3$. In a 3 mL Young NMR tube, 0.25 mmol of Et_3SiH (38 μL) was mixed with 0.6 mL of benzene-d_6. A combination of catalyst **1a** (1.5 mg, 0.0025 mmol) or **1b** (2.1 mg, 0.0025 mmol) and $B(C_6F_5)_3$ (2.0 mg, 0.0038 mmol) was then put on the top of the tube, avoiding early mixing with the hydrosilane before charging CO_2. The N_2 atmosphere was replaced with 1.0 bar of CO_2 using a freeze−pump−thaw cycle. Mixing all the components afforded immediately a light yellow solution. The mixture was kept at 80 °C, and the reaction progress was monitored by NMR spectroscopy. The color of solution gradually turned darker and eventually became purple. Alternatively, in a 50 mL autoclave vessel, **4a** (6.0 mg, 0.005 mmol) or **3a** (6.0 mg, 0.0025 mmol) was mixed with 0.5 mmol of Et_3SiH (76 μL) in 6 mL of benzene-d_6. Next, 5 bar of CO_2 was charged, and the reaction was kept at 80 °C for 13 h. The TON and TOF values were determined on the basis of the consumption of the hydrosilane. The composition of the products was determined by ^1H NMR and GC-MS. Characteristic NMR resonances:

$(Et_3SiO)_2CH_2$ ***(7).*** ^1H NMR (300.08 MHz, benzene-d_6, ppm): δ 5.07 (s), 1.05 (t, J = 9 Hz, CH_3), 0.67 (q, J = 6 Hz, $SiCH_2$). ^{29}Si NMR (90 MHz, benzene-d_6, ppm): δ 18.90 (s).

Et_3SiOCH_3 ***(9).*** ^1H NMR (300.08 MHz, benzene-d_6, ppm): δ 3.32 (s).

Hydrogenation of CO_2 Catalyzed by 1/$B(C_6F_5)_3$ in the Presence of Bases. In a 50 mL autoclave vessel, 0.005 mmol of [Re] (**1a**, 3.1 mg; **1b**, 4.3 mg; **3a**, 5.9 mg; **4a**, 5.9 mg) and 0.01 mmol of $B(C_6F_5)_3$ (5.4 mg) were mixed with 1.0 mmol of base (TMP, 170 μL; $HNiPr_2$, 140 μL; NEt_3, 150 μL; $HNCy_2$, 200 μL; $PtBu_3$, 250 μL; $HN(SiMe_3)_2$, 208 μL; 2,4,6-tri-*tert*-butylpyridine, 250 mg) in 1 mL of solvent (THF or chlorobenzene). Afterward the autoclave was charged with 20 bar of CO_2 and 40 bar of H_2. The mixture was kept at 80 °C for overnight. After the resultant solution cooled to room temperature, 10 μL of DMF (0.13 mmol) was added as an internal standard. An aliquot of the mixture (50 μL) was mixed in 0.5 mL of D_2O or $CDCl_3$ and examined by ^1H NMR spectroscopy. The yield was calculated by integration of the signal of the formato proton (δ 8.5, s) and that of DMF (δ 7.9, s). After the solvent was removed, the residue was washed with Et_2O (3 × 2 mL) and dried, giving off-white solids, which were identified to be the formate salts.

$[H\text{-}TMP]^+[O{-}CH{=}O]^-$ ***(11).*** Isolated: 37 mg, 20% yield. ^1H NMR (300.08 MHz, D_2O, ppm): δ 8.44 (s, 1 H, CHO), 1.75 (m, 2 H), 1.65 (m, 4 H), 1.39 (s, 12 H). ^1H NMR (300.08 MHz, $CDCl_3$, ppm): δ 8.70 (s, 1 H, CHO), 3.75 (s, 2H, NH), 2.17 (m, 2 H), 1.69 (m, 4 H), 1.45 (s, 12 H). ^{13}C NMR (75.47 MHz, D_2O, ppm): δ 171.4 (s), 57.2 (s), 34.9 (s), 27.1 (s), 16.1 (s). IR (cm^{-1}, ATR): 2947 (s), 2644 (s), 2596 (br), 2502 (br), 1587 (s, C=O). MS (ESI): m/z 142.2 ($[H\text{-}TMP]^+$). Anal. Calcd for $C_{10}H_{21}NO_2$ (187.16): C, 64.13; H, 11.30; N, 7.48. Found: C, 64.39; H, 11.25; N, 7.30.

$[H_2NiPr_2]^+[O{-}CH{=}O]^-$ ***(16).*** Isolated: 18 mg, 12% yield. ^1H NMR (300.08 MHz, $CDCl_3$, ppm): δ 8.58 (s, 1 H, CHO), 3.75 (br, 2H, NH), 3.42 (m, $^3J_{HH}$ = 6 Hz, 2H), 1.44 (d, $^3J_{HH}$ = 6 Hz, 12H). ^{13}C NMR (75.47 MHz, $CDCl_3$, ppm): δ 168.1 (s), 47.3 (s), 19.2 (s). IR (cm^{-1}, ATR): 2979 (s), 2864 (br), 2676 (s), 2492 (br), 1626 (s, C=O), 1555 (s). MS (ESI): m/z 102.4 ($[H_2NiPr_2]^+$).

$[H_2NCy_2]^+[O{-}CH{=}O]^-$ ***(17).*** Isolated: 30 mg, 13% yield. ^1H NMR (300.08 MHz, D_2O, ppm): δ 8.31 (s, 1 H, CHO), 3.06 (m, 2H, N−CH), 1.16−1.91 (m, 20 H). ^1H NMR (300.08 MHz, $CDCl_3$, ppm): δ 8.60 (s, 1 H, CHO), 3.74 (br, 2H, NH), 3.00 (m, 2H, N−CH), 1.23−2.09 (m, 20H). ^{13}C NMR (75.47 MHz, D_2O, ppm): δ 171.4 (s), 53.6 (s), 29.9 (s), 25.2 (s), 24.5 (s). ^{13}C NMR (75.47 MHz, $CDCl_3$, ppm): δ 168.1 (s), 52.8 (s), 29.2 (s), 25.1 (s), 24.8 (s). IR (cm^{-1}, ATR):

dx.doi.org/10.1021/ja402381d | J. Am. Chem. Soc. 2013, 135, 7751−7760

2936 (s), 2857(s), 2756 (s), 2671 (s), 1630 (s, C═O), 1548 (s). MS (ESI): m/z 182.1 ($[H_2NCy_2]^+$). Anal. Calcd for $C_{13}H_{25}NO_2$ (227.19): C, 68.68; H, 11.08; N, 6.16. Found: C, 68.72; H, 10.98; N, 6.05.

Computational Methods. All calculations were performed with the Gaussian03 program package[27] using the functional B3LYP[28] in combination with the Stuttgart/Dresden effective core potentials (SDD) basis set[29] for Re and the standard 6-31+G(d)[30] for the remaining atoms. Sums of electronic and zero-point energies are taken as relative energies.

Crystallographic Studies of Compounds 3a and 11. Single-crystal X-ray diffraction data were collected at 183(2) K on an Xcalibur diffractometer (Agilent Technologies, Ruby CCD detector) using a single-wavelength Enhance X-ray source with Mo Kα radiation (λ = 0.71073 Å) for **3a** and on a Supernova area-detector diffractometer using a high-intensity copper X-ray microsource (λ = 1.54184 Å) for **11**.[31] The selected suitable single crystals were mounted using polybutene oil on the top of a glass fiber fixed on a goniometer head and immediately transferred to the diffractometer. Pre-experiment, data collection, data reduction, and analytical absorption corrections[32] were performed with the program suite CrysAlis^{Pro}.[31] The crystal structures were solved with SHELXS97[33] using direct methods. The structure refinements were performed by full-matrix least-squares on F^2 with SHELXL97.[33] All programs used during the crystal structure determination process are included in the WINGX software.[34] PLATON[35] was used to check the result of the X-ray analyses. For more details about the refinements, see the *_exptl_special_details* and *iucr_refine_instructions_details* sections in the crystallographic information files (CIF, Supporting Information). CCDC-927599 (for **3a**) and CCDC-927600 (for **11**) contain the supplementary crystallographic data for this paper. These data can be obtained free of charge from The Cambridge Crystallographic Data Centre via www.ccdc.cam.ac.uk/data_request/cif.

■ ASSOCIATED CONTENT

Ⓢ Supporting Information

Crystallographic details and CIF files for **3a** and **11**; computational details; complete ref 27; and NMR spectra for CO_2 activation and reduction courses. This material is available free of charge via the Internet at http://pubs.acs.org.

■ AUTHOR INFORMATION

Corresponding Author

hberke@aci.uzh.ch

Notes

The authors declare no competing financial interest.

■ ACKNOWLEDGMENTS

Financial support from the Swiss National Science Foundation, Lanxess AG, Leverkusen, Germany, the Funds of the University of Zurich, the DFG, and SNF within the project "Forschergruppe 1175—Unconventional Approaches to the Activation of Dihydrogen" is gratefully acknowledged.

■ REFERENCES

(1) (a) Angamuthu, R.; Byers, P.; Lutz, M.; Spek, A. L.; Bouwman, E. *Science* **2010**, *327*, 313. (b) Das Neves Gomes, C.; Jacquet, O.; Villers, C.; Thuery, P.; Ephritikhine, M.; Cantat, T. *Angew. Chem., Int. Ed.* **2012**, *51*, 187. (c) Lewis, N. S.; Nocera, D. G. *Proc. Natl. Acad. Sci. U.S.A.* **2006**, *103*, 15729. (d) Olah, G. A. *Angew. Chem., Int. Ed.* **2005**, *44*, 2636. (e) Olah, G. A.; Prakash, G. K. S.; Goeppert, A. *J. Org. Chem.* **2009**, *74*, 487.

(2) For M/H_2: (a) Gassner, F.; Leitner, W. *J. Chem. Soc., Chem. Commun.* **1993**, 1465. (b) Jessop, P. G.; Ikariya, T.; Noyori, R. *Chem. Rev.* **1995**, *95*, 259. (c) Jessop, P. G.; Ikariya, T.; Noyori, R. *Nature* **1994**, *368*, 231. (d) Munshi, P.; Main, A. D.; Linehan, J. C.; Tai, C. C.; Jessop, P. G. *J. Am. Chem. Soc.* **2002**, *124*, 7963. (e) Himeda, Y.; Onozawa-Komatsuzaki, N.; Sugihara, H.; Kasuga, K. *Organometallics* **2007**, *26*, 702. (f) Tanaka, R.; Yamashita, M.; Nozaki, K. *J. Am. Chem. Soc.* **2009**, *131*, 14168. (g) Federsel, C.; Boddien, A.; Jackstell, R.; Jennerjahn, R.; Dyson, P. J.; Scopelliti, R.; Laurenczy, G.; Beller, M. *Angew. Chem., Int. Ed.* **2010**, *49*, 9777. (h) Cokoja, M.; Bruckmeier, C.; Rieger, B.; Herrmann, W. A.; Kühn, F. E. *Angew. Chem., Int. Ed.* **2011**, *50*, 8510. (i) Langer, R.; Diskin-Posner, Y.; Leitus, G.; Shimon, L. J. W.; Ben-David, Y.; Milstein, D. *Angew. Chem., Int. Ed.* **2011**, *50*, 9948. (j) Huff, C. A.; Sanford, M. S. *J. Am. Chem. Soc.* **2011**, *133*, 18122. (k) Wesselbaum, S.; vom Stein, T.; Klankermayer, J.; Leitner, W. *Angew. Chem., Int. Ed.* **2012**, *51*, 7499.

(3) For M/silane: (a) Eisenschmid, T. C.; Eisenberg, R. *Organometallics* **1989**, *8*, 1822. (b) Matsuo, T.; Kawaguchi, H. *J. Am. Chem. Soc.* **2006**, *128*, 12362. (c) Park, S.; Bezier, D.; Brookhart, M. *J. Am. Chem. Soc.* **2012**, *134*, 11404. (d) Riduan, S. N.; Zhang, Y. *Dalton Trans.* **2010**, *39*, 3347. (e) Deglmann, P.; Ember, E.; Hofmann, P.; Pitter, S.; Walter, O. *Chem.—Eur. J.* **2007**, *13*, 2864. (f) Jessop, P. G.; Ikariya, T.; Noyori, R. *Chem. Rev.* **1999**, *99*, 475.

(4) For M/borane: (a) Laitar, D. S.; Müller, P.; Sadighi, J. P. *J. Am. Chem. Soc.* **2005**, *127*, 17196. (b) Chakraborty, S.; Zhang, J.; Krause, J. A.; Guan, H. *J. Am. Chem. Soc.* **2010**, *132*, 8872. (c) Huang, F.; Zhang, C.; Jiang, J.; Wang, Z.-X.; Guan, H. *Inorg. Chem.* **2011**, *50*, 3816. (d) Bontemps, S.; Vendier, L.; Sabo-Etienne, S. *Angew. Chem., Int. Ed.* **2012**, *51*, 1671.

(5) For NHCs: (a) Lavigne, F.; Maerten, E.; Alcaraz, G.; Branchadell, V.; Saffon-Merceron, N.; Baceiredo, A. *Angew. Chem., Int. Ed.* **2012**, *51*, 2489. (b) Kayaki, Y.; Yamamoto, M.; Ikariya, T. *Angew. Chem., Int. Ed.* **2009**, *48*, 4194. (c) Riduan, S. N.; Zhang, Y.; Ying, J. Y. *Angew. Chem., Int. Ed.* **2009**, *48*, 3322. (d) Gu, L.; Zhang, Y. *J. Am. Chem. Soc.* **2010**, *132*, 914. (e) Jacquet, O.; Des Neves Gomes, C.; Ephritikhine, M.; Cantat, T. *J. Am. Chem. Soc.* **2012**, *134*, 2934.

(6) For silylium: Schäfer, A.; Saak, W.; Haase, D.; Müller, T. *Angew. Chem., Int. Ed.* **2012**, *51*, 2981.

(7) For $[Et_2Al]^+$: Khandelwal, M.; Wehmschulte, R. J. *Angew. Chem., Int. Ed.* **2012**, *51*, 1.

(8) Reviews of FLPs: (a) Stephan, D. W.; Erker, G. *Angew. Chem., Int. Ed.* **2010**, *49*, 46. (b) Stephan, D. W. *Dalton Trans.* **2009**, 3129.

(9) Special issue on "Frustrated Lewis Pairs". *Dalton Trans.* **2012**, *41*, 8999–9045.

(10) For B/P: (a) Mömming, C. M.; Otten, E.; Kehr, G.; Fröhlich, R.; Grimme, S.; Stephan, D. W.; Erker, G. *Angew. Chem., Int. Ed.* **2009**, *48*, 6643. (b) Hounjet, L. J.; Caputo, C. B.; Stephan, D. W. *Angew. Chem., Int. Ed.* **2012**, *51*, 4714. (c) Peuser, I.; Neu, R. C.; Zhao, X.; Ulrich, M.; Schirmer, B.; Tannert, J. A.; Kehr, G.; Fröhlich, R.; Grimme, S.; Erker, G.; Stephan, D. W. *Chem.—Eur. J.* **2011**, *17*, 9640. (d) Harhausen, M.; Fröhlich, R.; Kehr, G.; Erker, G. *Organometallics* **2012**, *31*, 2801.

(11) For B/N: (a) Ashley, A. E.; Thompson, A. L.; OHare, D. *Angew. Chem., Int. Ed.* **2009**, *48*, 9839. (b) Berkefeld, A.; Piers, W. E.; Parvez, M. *J. Am. Chem. Soc.* **2010**, *132*, 10660. (c) Khalimon, A. Y.; Piers, W. E.; Blackwell, J. M.; Michalak, D. J.; Parvez, M. *J. Am. Chem. Soc.* **2012**, *134*, 9601. (d) Voss, T.; Mahdi, T.; Otten, E.; Fröhlich, R.; Kehr, G.; Stephan, D. W.; Erker, G. *Organometallics* **2012**, *31*, 2367.

(12) For Al/P: (a) Menard, G.; Stephan, D. W. *J. Am. Chem. Soc.* **2010**, *132*, 1796. (b) Menard, G.; Stephan, D. W. *Angew. Chem., Int. Ed.* **2011**, *50*, 8396. (c) Appelt, C.; Westenberg, H.; Bertini, F.; Ehlers, A. W.; Slootweg, J. C.; Lammertsma, K.; Uhl, W. *Angew. Chem., Int. Ed.* **2011**, *50*, 3925. (d) Boudreau, J.; Courtemanche, M. A.; Fontaine, F. G. *Chem. Commun.* **2011**, *47*, 11131. (e) Menard, G.; Stephan, D. W. *Angew. Chem., Int. Ed.* **2012**, *51*, 8272.

(13) For M–H/CO_2: (a) Pu, L. S.; Yamamoto, A.; Ikeda, S. *J. Am. Chem. Soc.* **1968**, *90*, 3896. (b) Darensbourg, D. J. *Inorg. Chem.* **2010**, *49*, 10765. (c) Musashi, Y.; Sakaki, S. *J. Am. Chem. Soc.* **2000**, *122*, 3867. (d) Yin, X.; Moss, J. R. *Coord. Chem. Rev.* **1999**, *181*, 27. (e) Gibson, D. H. *Coord. Chem. Rev.* **1999**, *185–186*, 335. (f) Yin, C.; Xu, Z.; Yang, S. Y.; Ng, S. M.; Wong, K. Y.; Lin, Z.; Lau, C. P. *Organometallics* **2001**, *20*, 1216.

(14) For transition-metal-involved FLPs: (a) Chapman, A. M.; Haddow, M. F.; Wass, D. F. *J. Am. Chem. Soc.* **2011**, *133*, 18463. (b) Sgro, M. J.; Stephan, D. W. *Angew. Chem., Int. Ed.* **2012**, *51*, 11343.

(15) (a) Jiang, Y.; Blacque, O.; Fox, T.; Frech, C. M.; Berke, H. *Chem.—Eur. J.* **2009**, *15*, 2121. (b) Jiang, Y.; Blacque, O.; Fox, T.; Frech, C. M.; Berke, H. *Organometallics* **2009**, *28*, 5493. (c) Jiang, Y.; Blacque, O.; Fox, T.; Frech, C. M.; Berke, H. *Organometallics* **2009**, *28*, 4670. (d) Jiang, Y.; Blacque, O.; Fox, T.; Frech, C. M.; Berke, H. *Chem.—Eur. J.* **2010**, *16*, 2240. (e) Jiang, Y.; Hess, J.; Fox, T.; Berke, H. *J. Am. Chem. Soc.* **2010**, *132*, 18233.
(16) Saverio, A. D.; Focante, F.; Camurati, I.; Resconi, L.; Beringhelli, T.; D'Alfonso, G.; Donghi, D.; Maggioni, D.; Mercandelli, P.; Sironi, A. *Inorg. Chem.* **2005**, *44*, 5030.
(17) For Os: (a) Kuhlman, R.; Streib, W. E.; Huffman, J. C.; Caulton, K. G. *J. Am. Chem. Soc.* **1996**, *118*, 6934. (b) Esteruelas, M. A.; Lopez, A. M.; Onate, E.; Royo, E. *Organometallics* **2005**, *24*, 5780. For Rh: (c) Cheliatsidou, P.; White, D. F. S.; de Bruin, B.; Reek, J. N. H.; Cole-Hamilton, D. J. *Organometallics* **2007**, *26*, 3265.
(18) (a) Höck, J.; Jacobsen, H.; Schmalle, H. W.; Artus, G. R. J.; Fox, T.; Amor, J. I.; Bäth, F.; Berke, H. *Organometallics* **2001**, *20*, 1533. (b) Zhao, Y.; Schmalle, H. W.; Fox, T.; Blacque, O.; Berke, H. *Dalton Trans.* **2006**, 73.
(19) Gusev, D.; Llamazares, A.; Artus, G.; Jacobsen, H.; Berke, H. *Organometallics* **1999**, *18*, 75.
(20) Jiang, Y.; Blacque, O.; Fox, T.; Berke, H. *J. Am. Chem. Soc.* **2013**, *135*, 4088.
(21) Landwehr, A.; Dudle, B.; Fox, T.; Blacque, O.; Berke, H. *Chem.—Eur. J.* **2012**, *18*, 5701.
(22) (a) Noyori, R.; Ohkuma, T. *Angew. Chem., Int. Ed.* **2001**, *40*, 40. (b) Noyori, R.; Yamakawa, M.; Hashiguchi, S. *J. Org. Chem.* **2001**, *66*, 7931. (c) Morris, R. H. *Chem. Soc. Rev.* **2009**, *38*, 2282. (d) Morris, R. H. *Coord. Chem. Rev.* **2008**, *252*, 2381. (e) Clapham, S. E.; Hadzovic, A.; Morris, R. H. *Coord. Chem. Rev.* **2004**, *248*, 2201. (f) Gruetzmacher, H. *Angew. Chem., Int. Ed.* **2008**, *47*, 1814. (g) Ingleson, M. J.; Brayshaw, S. K.; Mahon, M. F.; Ruggiero, G. D.; Weller, A. S. *Inorg. Chem.* **2005**, *44*, 3162. (h) Kubas, G. J. *Adv. Inorg. Chem.* **2004**, *56*, 127. (i) Yi, C. S.; Lee, D. W.; He, Z.; Rheingold, A. L.; Lam, K.-C.; Concolino, T. E. *Organometallics* **2000**, *19*, 2909. (j) Heinekey, D. M.; Lledos, A.; Lluch, J. M. *Chem. Soc. Rev.* **2004**, *33*, 175.
(23) Ilyin, P. V.; Pankova, A. S.; Kuznetsov, M. A. *Synthesis* **2012**, *44*, 1353.
(24) Jeffrey, G. A. *An introduction to hydrogen bonding*; Oxford University Press: Oxford, UK, 1997.
(25) (a) Heinekey, D. M.; Millar, J. M.; Koetzle, T. F.; Payne, N. G.; Zilm, K. W. *J. Am. Chem. Soc.* **1990**, *112*, 909. (b) Dudle, B.; Rajesh, K.; Blacque, O.; Berke, H. *J. Am. Chem. Soc.* **2011**, *133*, 8168.
(26) (a) Maseras, F.; Lledos, A.; Clot, E.; Eisenstein, O. *Chem. Rev.* **2000**, *100*, 601. (b) Kubas, G. J. *Chem. Rev.* **2007**, *107*, 4152.
(27) Frisch, M. J.; et al. *Gaussian 03*, revision D.01; Gaussian, Inc.: Wallingford, CT, 2003.
(28) (a) Becke, A. D. *J. Chem. Phys.* **1993**, *98*, 5648. (b) Lee, C.; Yang, W.; Parr, R. G. *Phys. Rev. B* **1988**, *37*, 785. (c) Miehlich, B.; Savin, A.; Stoll, H.; Preuss, H. *Chem. Phys. Lett.* **1989**, *157*, 200.
(29) Dunning, T. H., Jr.; Hay, P. J. *Modern Theoretical Chemistry*; Plenum: New York, 1976.
(30) Ditchfield, R.; Hehre, W. J.; Pople, J. A. *J. Chem. Phys.* **1971**, *54*, 724.
(31) Agilent Technologies (formerly Oxford Diffraction), Yarnton, England, 2011.
(32) Clark, R. C.; Reid, J. S. *Acta Crystallogr. A* **1995**, *51*, 887.
(33) Sheldrick, G. *Acta Crystallogr. A* **2008**, *64*, 112.
(34) Farrugia, L. *J. Appl. Crystallogr.* **1999**, *32*, 837.
(35) Spek, A. L. *J. Appl. Crystallogr.* **2003**, *36*, 7.